ESTIMATING SHEAR STRENGTH OF RC AND PRC MEMBER WITH FIBER SHEETS

(Translation from Proceeding of JSCE, No.655/V-48, August 2000)


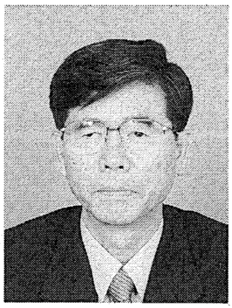
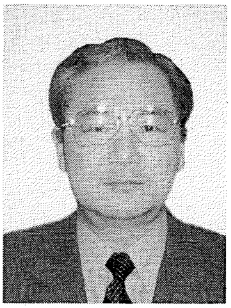

Kenji IZUMO　　Noboru SAEKI　　Hiroshi OHNUMA

Experiments are carried out on RC members in which the shear crack location is limited by notches so as to estimate the shear strength of RC members with fiber sheets. In these experiments, we investigate effective bond area of the fiber sheets and shear strength. It is possible to estimate the improvement obtained by using the fiber sheets by incorporating the effective bond area into the equation for bond strength between fiber sheet and concrete as presented in an earlier paper by the authors. Moreover, we investigate shear strengthening of RC beams using fiber sheets and the strengthening of RC beams using prestressing fiber sheets. As a result of these experiments, the shear-strengthening effects of fiber sheets and prestressing force are clarified. Moreover, we are able to estimate the experimental values by calculation.

Key Words: aramid fiber sheet, carbon fiber sheet, shear strengthening, RC member, prestressing force

Kenji IZUMO is a Research Associate in the Department of Civil Engineering at Hokkaido University, Sapporo, Japan. He obtained his D.Eng. from Hokkaido University in 1999. His research interests strengthening concrete structure using fiber sheets. He is a member of JSCE.

Noboru SAEKI is a Professor in the Department of Civil Engineering at Hokkaido University. He obtained his D.Eng. from Hokkaido University in 1972. His research interests FRP, eco-concrete, and reinforced concrete members subject to torsion. He is a member of JSCE.

Hiroshi OHNUMA is a Professor in the Department of Civil Engineering at Hokkaido University. He obtained his D.Eng. from Hokkaido University in 1985. His research interests high-strength concrete under triaxial compression and impact response analysis reinforced concrete members. He is a member of JSCE.

1. INTRODUCTION

It was believed that concrete structures had semipermanent durability, but concrete structures have recently been found to suffer damage and deterioration as a result of salt attack and other factors such as increasing traffic and traffic loading. There is also a need to improve the safety of existing concrete structures in light of the damage caused by the Hanshin-Awaji earthquake. It is not possible to close such concrete structures to do the work because they often important social roles. Therefore, the effective rehabilitation and strengthening of concrete structures have became important issues.

Studies on improving the safety of existing concrete structures have been very active. One of the many strengthening methods is the use of fiber sheets to add strength; this method has the advantage of being comparatively easy. The increased dead load is of little consequence because fiber sheets are lighter than steel. Fiber sheets also have good durability. However, when shear cracking takes place, the RC members with fiber sheet covering may fail by peeling of the fiber sheets from the concrete surface. The bond behaviour between fiber sheets and concrete in this situation has yet to be clarified.

In an earlier paper [1], we showed that it is possible to estimate the strength of the bond between fiber sheets and concrete under uni-axial tensile stress. Research relating to the shear strength of RC members with fiber sheets is active, and includes a paper by the authors [2] and many by others [3],[4],[5],[6],[7]. However, the estimation of shear strength has yet to be clarified for RC members that fail by peeling of fiber sheets from the concrete surface.

In one earlier work [3], the shear strength of RC members with fiber sheets was obtained by investigating bond behavior. The effective bond area of fiber sheets has also been investigated in the hope of improving the shear strength. However, in this earlier work, bond strength is calculated by presumed value. In this paper, bond strength is estimated by uni-axial tensile tests.

In other papers [4],[6], the shear strength of RC members with fiber sheets was obtained not by investigating bond behavior but from the tensile strength of fiber sheet. As a consequence, when RC members failed by peeling of fiber sheets from the concrete surface, the shear strength was over-estimated. A reduction coefficient was used to correct this in one paper [4].
In this paper, two experiments are carried out: a model experiment with RC members and an experiment of RC beams with stirrups.

In the model experiment, RC members without stirrups were used. Fiber sheeting was bond to the webs of RC members. Notches were created in the RC members to limit the location of shear cracks. We investigated the area of fiber sheeting that acts to resist shear cracking; namely, the effective bond area of the fiber sheets. The shear capacity of the fiber sheets was estimated by applying the effective bond area to the equation for bond strength between fiber sheets and concrete, as presented in an earlier paper [1].

In the experiments with actual RC beams, stirrups were used. Fiber sheeting was bonded to the webs of the beams. We investigated the shear-strengthening effect of the fiber sheeting. Further, we investigated the effect of prestressing force into the fiber sheets. In same earlier papers [8],[9], FRP plates were bonded as tendons to the bottom of the RC beams. In this paper, fiber sheets were bonded as tendons to the webs of RC beams.

2. OUTLINE OF EXPERIMENTS

(1) Materials

The properties of the carbon and aramid fiber sheets used in the experiments are shown in Table 1. These are experimental values obtained in accordance with the JIS standard (JIS K 7073). The thickness of the fiber sheeting is calculated by aerial weight/density.

These fiber sheets are biaxial, and the ratio of vertical to horizontal fibers is 1 : 1. The reasons for adopting biaxial fiber sheeting are as follows: the fiber sheets are bonded to the webs of the beams, and the vertical fibers act as stirrups while the horizontal fibers act as tendons.

Table 1 Properties of Fiber Sheets

Series	96		97	
Type of fiber sheet	CFS96	AFS96	CFS97	AFS97
Aerial weight (g/m^2)(vertical : horizontal fiber)	400(200:200)	400(200:200)	600(300:300)	470(235:235)
Density (g/m^3)	1.79	1.39	1.80	1.39
Thickness (mm)	0.112	0.144	0.167	0.169
Ultimate tensile strength (N/mm^2)	3879	2493	3115	2134
Young's modulus (kN/mm^2)	242	86	222	73
Ultimate elongation (%)	2.1	3.1	1.6	3.3

A primer and epoxy resin are used to effectively bond the sheets to the concrete.

(2) Model RC Members

RC members with fiber sheets bonded to the webs were notched for estimation of shear strength. The notches were created so as to limit the location of shear cracks, and we investigated the area of fiber sheeting that resists shear cracking; namely, the effective bond area of the fiber sheets. With the location of shear cracks limited by the notch, the bond area of the fiber sheets that resists shear cracking is easy to obtain.

The fiber sheets were bonded as follows:
1) The concrete surface is sanded by a disc sander to remove coating material.
2) Primer is spread on the concrete and allowed to cure for about a day.
3) Fiber sheets are bonded to the concrete with epoxy resin and allowed to cure for one week.

An outline of the specimens is given in Fig. 1. Steel bars of D13 (13 mm in diameter; yield point 345 N/mm^2) in series 96-S and D16 (16 mm in diameter; yield point 345 N/mm^2) in series 97-S were used as longitudinal tensioning bars. Stirrups were not used because shear failure was assumed. The characteristics of the various specimens are given in Table 2.

Three-point loading over a 600mm span was used.

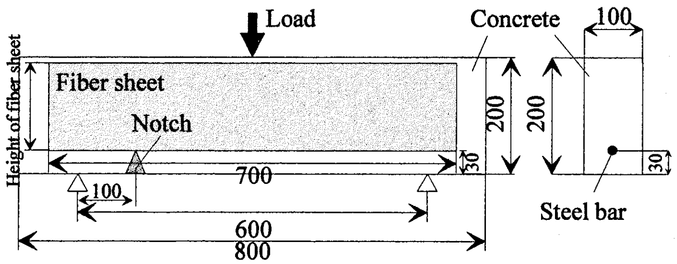

Fig. 1 Outline of Specimen Used for Model Experiment

(3) RC Beams

An outline of the specimens and the strain gage locations are given in Fig. 2. The RC beams have a T-shape section. Steel bars of D19 (19 mm in diameter; yield point 345 N/mm^2) in series 96 and D29 (29 mm in diameter; yield point 345 N/mm^2) in series 97 are used as longitudinal tensioning bars. D6 (6 mm in diameter, yield point 295 N/mm^2) steel bars are used as compression bars and stirrups in both series. The stirrup spacing is 200mm. Fiber sheeting is bonded to the web of the RC beams as shown in Fig. 2. In these experiments, Three-point loading over a 1700 mm span was used.

Table 2 Characteristics of the Model Experiment Specimens

Specimen	Type of fiber sheet	Height of fiber sheet (mm)	Compressive strength of concrete (N/mm^2)	Tensile strength of concrete (N/mm^2)	Young's modulus of concrete (N/mm^2)	Failure
96-S-N	-	-	24.9	2.3	28600	S
96-S-A	AFS96	150	25.6	2.2	22900	PS
96-S-C	CFS96	150	25.6	2.2	22900	PS
97-S-N	-	-	27.5	2.2	22100	S
97-S-A	AFS97	150	27.5	2.2	22100	PS
97-S-C	CFS97	150	27.5	2.2	22100	PS
97-S-N-H	-	-	23.9	1.9	22700	S
97-S-A-H	AFS97	85	23.9	1.9	22700	PS
97-S-C-H	CFS97	85	23.9	1.9	22700	PS

S: Shear failure; PS: Shear failure due to peeling of fiber sheet

The strain gage locations are also shown in Fig. 2. Strain gages, R1-R9, were bonded to the fiber sheeting covering the stirrups. Strain gages S1-S3 were bonded to the stirrups. Strain gages T1-T2 were bonded to the longitudinal tensioning bars. Strain gage C1 was bonded to the comprsion bar.

The Major characteristics of these RC beams are given in Table 3, where the prestressing force is the value per a sheet.

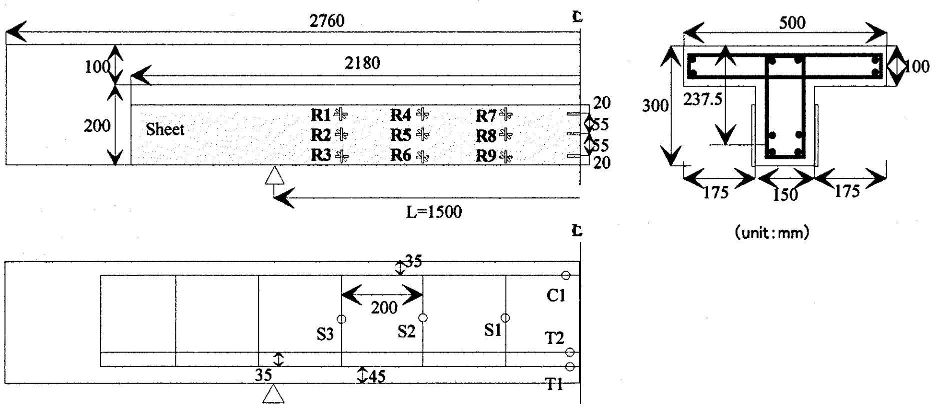

Fig. 2 Outline of RC Beam Specimens and Location of Strain Gages

Table 3 Properties of RC Beams

Specimen	Type of fiber sheet	Tension Steel bar	Compressive strength of concrete (N/mm^2)	Young's modulus of concrete (N/mm^2)	Prestressing force (kN)	Failure
96-N-0	-	D19	46.4	28300	-	S
96-C-0	CFS96	D19	52.0	28000	0	PS
96-C-15	CFS96	D19	40.3	22000	15×2	PS
96-A-0	AFS96	D19	60.3	29400	0	PS
96-A-15	AFS96	D19	42.5	28400	15×2	PS
97-N-0	-	D29	42.6	26600	-	S
97-A-0	AFS97	D29	45.7	25300	0	PS

S: Shear failure; PS: Shear failure due to peeling of fiber sheet

(4) Applying of Prestressing Force to Fiber Sheeting

The process of applying prestressed force to the fiber sheeting is shown in Fig. 3. It is a four-step process.

First, the RC beam surface is prepared with a disc sander and primer coating (Fig. 3a), and, the RC beam is cured for about a day.

Secondly, the fiber sheeting is bonded at one end only and held in place with metal fittings (Fig. 3b). Both sides of the beam are treated in this way. The RC beams were cured for about a day.

Thirdly, the fiber sheeting is epoxy-bonded to the web of the RC beams from end to end. The attachment frames of the hydraulic jacks were set at other end. Then the fiber sheet end were wrapped around a roller to fix it. (Fig. 3c), and the roller is fixed with stopper.

Lastly, the hydraulic jacks are set on the attachment frames and the tensioning bars and roller are made to connect (Fig. 3d). Prestressing force is induced into the fiber sheeting by drawing back the rollers with the hydraulic jacks. The fiber sheeting are held under tension until the epoxy resin hardened, in about a week. The prestressing equipment is then removed, and the RC beams used for experiments at once. (Patent application No. 038545 in Japan)

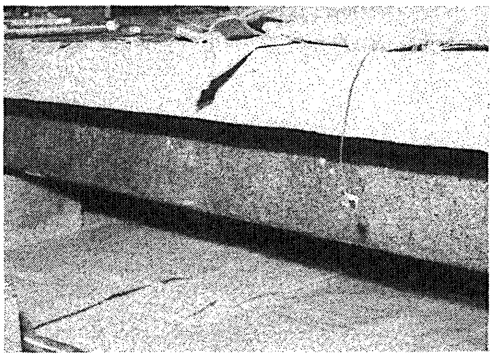

(a) Groundwork Processing

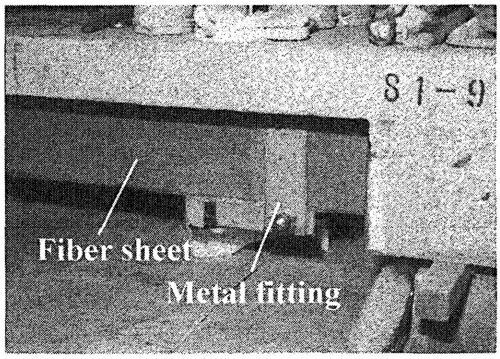

(b) Fixing Edge of Fiber Sheet

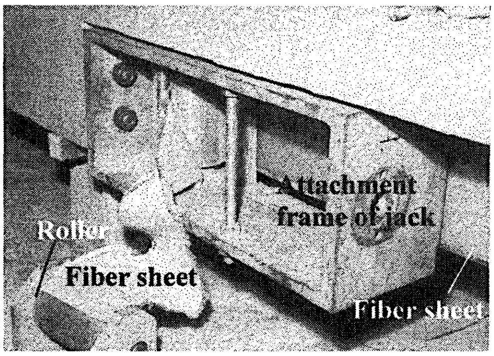

(c) Bonding Fiber Sheet to Concrete

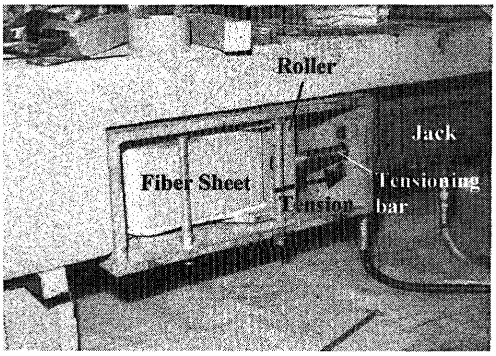

(d) Adding Prestressing Force to Fiber Sheet

Fig. 3 Process of Adding Prestressing Force to Fiber Sheets

3. ESTIMATION OF SHEAR STRENGTH OF RC MEMBERS WITH FIBER SHEETS WITHOUT STIRRUP

(1) Process of Fiber Sheets Peeling

The process by which fiber sheets peel is illustrated in Fig. 4. Fig 4(a) and (c) are photographs of RC member failure. The crack initiated at the notch. Peeling took place from the upper edge of the fiber sheets. When peeling reached the half height of the fiber sheet, the RC member failed at the maximum load. Other specimens also failed by peeling of the fiber sheet from concrete surface after shear cracking.

The process of fiber sheet peeling is shown schematically in Fig. 4(b). After the fiber sheet peels off in the white area, the RC member fails. After the crack reaches the vicinity of the upper edge of the RC member, the upper edge of the fiber sheet begins to peel, as shown in Fig. 4(a) and (c). Thereafter, peeling extends in the direction of the arrow shown in Fig. 4(b). When peeling of the fiber sheets reaches the half height of the fiber sheet, the RC member fails at the maximum load. Reports of such a failure mode have been given in an earlier paper [3].

The load-displacement curve for 97-S-C-H is shown in Fig. 4(d). When load was 55kN, peeling of the fiber sheet was checked for the first time. However, it is difficult to accurately pinpoint the beginning of peeling since we confirm it by the sound made by tapping the fiber sheet. The point near 50kN that inclination of a curve is loose clearly is considered to be the time of the beginning of fiber sheet peeling.

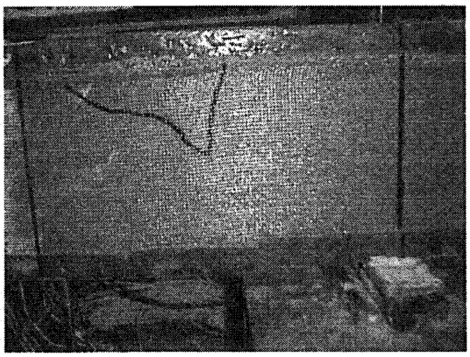

(a) Photograph of Shear Failure in 97-S-A

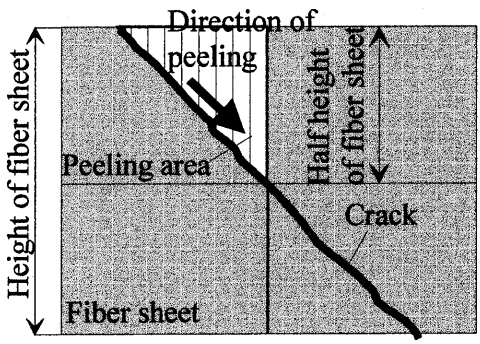

(b) Process of Peeling of Fiber Sheet

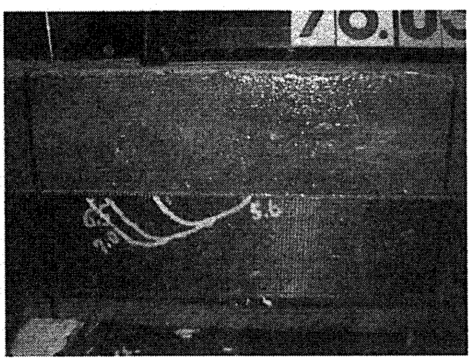

(c) Photograph of Shear Failure in 97-S-C-H

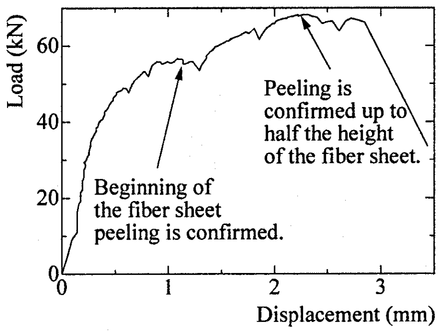

(d) Load-Displacement curve in 97-S-C-H

Fig. 4 Failure Process of RC Members

After peeling is confirmed, the load drops. The load rises again and a further section of fiber sheet peels off, this process is repeated with the load going down and up a number of times. When peeling reaches the half height of the fiber sheet, the load reaches a maximum of about 68kN. Afterwards, peeling progresses and the RC member fails.

Fiber sheeting is able to carry a load only in the direction of the fibers, but not away from the fiber direction. We consider that the force against shear cracks is shared by the axial direction and orthogonal direction. Comparing the axial and orthogonal fibers, short fibers have weak resistance to shearing cracks. Therefore, we only have to consider the orthogonal fibers because they are shorter than the axial ones.

Since tensile stress is caused by shear stress at the crack, it seems that the upper or lower edge of the fiber sheet is most susceptible to stress. The lower edge of the fiber sheet is supported by fiber sheet resisting the stress above it, whereas the upper edge does not have benefit. As a result, it seems that peeling of the fiber sheet begins from the upper edge.

The reason for peeling reaching the half height position at the moment of maximum loading is as follows. The shorter bond lying length across the crack always peels first because it is weak at resisting stress. Therefore, when peeling reaches the half height of the fiber sheet, the load is the maximum because the shorter bond length is the maximum.

(2) Estimation of Shear Strength for Fiber Sheets of RC Members without Stirrup

The equation for the bond strength between fiber sheet and concrete as given in our earlier paper [1] is,

$$B_{cal} = (a_1 \cdot f_c^{2/3} + a_2) \cdot L_f \cdot E_f \cdot B_f \cdot t_f \times 10^{-6} \quad \text{(kN)} \tag{1}$$

Where, $a_1 = 2.6$ for AFS
$a_1 = 2.9$ for CFS
$a_2 = 68.7$ for AFS
$a_2 = 11.5$ for CFS
f_c = compressive strength of concrete (N/mm^2)
E_f = young's modulus of fiber sheet (kN/mm^2)
b_f = bond width of fiber sheet (mm)
l_f = bond length of fiber sheet (mm)
t_f = thickness of fiber sheet (mm)
$L_f = L_e$ for $l_f \geqq L_e$
$L_f = \alpha(l_f)$ for $l_f < L_e$
$\alpha(l_f) = l_f \cdot (3.11 - 0.0420 l_f + 2.09 l_f^2 \times 10^{-4})$
$B_f = b_f$ for $b_f \geqq 80$
$B_f = \beta(b_f) \cdot b_f$ for $b_f < 80$
$\beta(b_f) = 1.818 - 0.0102 \cdot b_f$

In order to estimate Eq. (1), uni-axial tensile test was carried out on specimens shown in Fig. 5. In these uni-axial tensile specimens, the space between concretes is assumed to be the crack. Because the left end is strengthened by rolling the fiber sheet, the right end fails by peeling.

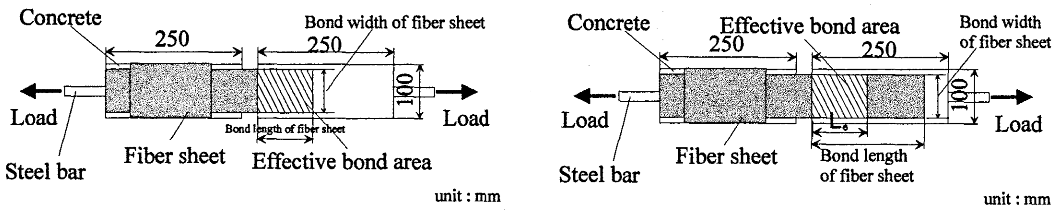

(a) Effective Bond Area for $l_f < L_e$ (b) Effective Bond Area for $l_f \geqq L_e$

Fig. 5 Outline of Specimens Under Uni-Axial Tensile Testing

In this paper, the effective area of the fiber sheet providing bonding between the fiber sheet and concrete is defined as the effective bond area. When the bond length is below the effective bond length L_e, the bond area becomes the effective bond area as shown in Fig. 5(a). Besides, when the bond length is greater than the effective bond length L_e, the bond between fiber sheet and concrete is of the same strength as in our earlier paper [1]. Therefore, when the bond length is greater than effective bond length L_e, the effective bond area is $b_f \times L_e$.

When this effective bond area is similarly applied to a shear crack, it will apply to the upper half in which the fiber sheet peels. However, it seems that the effective bond length L_e exists as well as under the uni-axial tensile stress. Therefore, the half height of the fiber sheet $h_f/2$ is divided as follows in cases where it is greater than the effective bond length L_e.

In the case of $h_f/2 < L_e$, the effective bond area which contributes to shear strength seems to be an upper right-angled triangle as shown in Fig. 6(a). Therefore, in these model experiments, a right-angled triangle of height $h_f/2$ and base $h_f/2 \cdot \tan\alpha$ was defined as the effective bond area of the fiber sheet.
In the case of $h_f/2 \geqq L_e$, the trapezoid with the height $L_e \cdot \sin\alpha$ and the sides $(h_f/2 - L_e)/\sin\alpha$, $h_f/2 \sin\alpha$ was defined as the effective bond area as shown in Fig. 6(b).

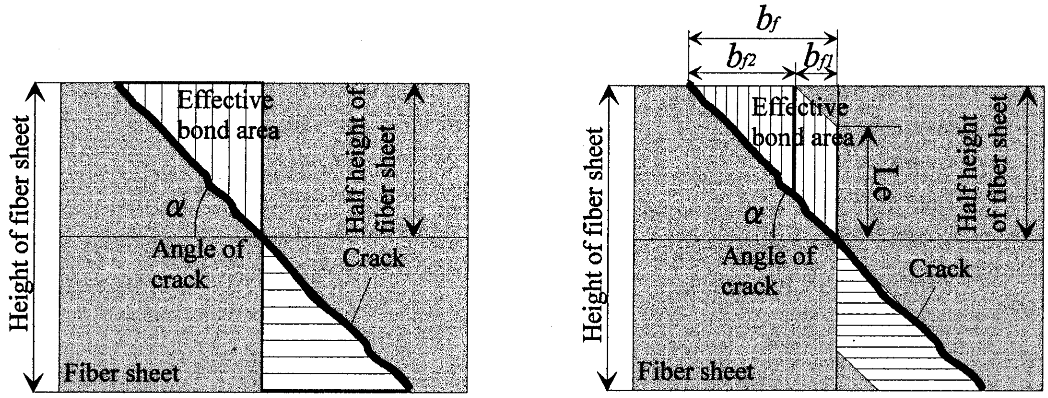

(a) Effective Bond Area Against Shear Crack for $h_f/2 < L_e$

(b) Effective Bond Area Against Shear Crack for $h_f/2 \geqq L_e$

Fig. 6 Process of Peeling of Fiber Sheet and Outline of Effective Bond Area

However, the effective bond area does not carry the load until the maximum load is reached because the fiber sheet in the effective bond area peels gradually. An area almost equivalent to the effective bond area exists under the height half of the fiber sheet as shown in Fig. 6(a) and (b). Because this area does not peel until the maximum load, it seems that this area carries the load.

When this effective bond area is applied to Eq. (1), the bond strength between fiber and concrete is estimated due to applying the effective bond area to bond length L_f and bond width B_f. The shear capacity of fiber sheets is estimated by truss theory as Eq. 2(a) in $h_f/2 < L_e$ and Eq. 2(b) in $h_f/2 \geqq L_e$. Where, the effective bond area is divided into the right-angled triangle and the parallelogram in $h_f/2 \geqq L_e$.

In the case of $h_f/2 < L_e (l_f < L_e)$,

$$V_{fd} = \frac{\int_0^{h_f/2} B_{cal} \cdot dl_f}{h_f/2} \cdot \frac{z}{d}$$
$$= (a_1 \cdot f^{2/3} + a_2) \cdot \gamma(h_f) \cdot E_f \cdot B_f \cdot t_f \cdot \frac{z}{d} \times 10^{-6} \tag{2a}$$

Where, $\gamma(h_f) = h_f \cdot (0.778 - 3.50 \cdot h_f \times 10^{-3} + 6.53 \cdot h_f^2 \times 10^{-6})$

In the case of $h_f/2 \geqq L_e(l_f \geqq L_e)$,

$$V_{fd} = [\frac{\int_0^{2 \cdot Le/2} B_{cal} \cdot dl_f}{h_f/2} + 100 \cdot (a \cdot f'^{2/3} + b) \cdot E_f \cdot B_{f1} \cdot t_f \times 10^{-6}] \cdot \frac{z}{d}$$

$$= (a_1 \cdot f'^{2/3} + a_2) \cdot [\gamma(2 \cdot L_e) \cdot B_{f2} + 100 \cdot B_{f1}] \cdot E_f \cdot t_f \cdot \frac{z}{d} \times 10^{-6} \tag{2b}$$

Where, $b_f = b_{f1} + b_{f2}$

$B_{f1} = b_{f1}$, $B_{f2} = b_{f2}$ for $b_f \geqq 80$

$B_{f1} = \beta(b_f) \cdot b_{f1}$, $B_{f2} = \beta(b_f) \cdot b_{f2}$ for $b_f < 80$

The angle of the crack is calculated using an equation given in an earlier paper [10].

In general, the pattern of shear failure is divided into shear compression and tension failure. However, the calculation method proposed here is not concerned with shear compression and tension failure according to the effective bond area to a shear crack. Therefore, this calculation method is possible to estimate the shear capacity of fiber sheet.

(3) Result of Experiment and Calculation

The specimens described in this paper failed after peeling of the fiber sheet. The shear crack initiated at the tip of the notch. By strengthening RC members with fiber sheeting, a shear strength improvement is seen, as also reported in the part. The shear capacity by experiment and as calculated using Eq. (2a) and (2b) is shown in Fig. 7 and Table 4. Although there is also some RC members which cannot be estimating experiment value greatly, it is possible to estimate by equation proposed in this paper. Besides, all past papers are based on experimental results for specimens bonded with one-directional fiber sheets in the orthogonal direction.

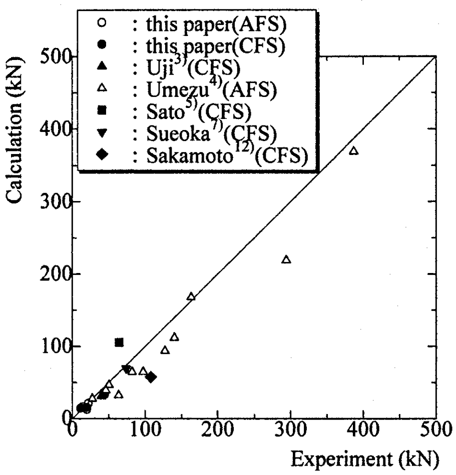

Fig. 7 Comparison of Calculation and Experiment

4. RESULTS OF RC BEAM EXPERIMENTS AND CONSIDERATION

(1) Failure Pattern

Photographs of failed RC beams, the crack characteristics and the area of peeling are shown in Fig. 8. The RC beams failed due to peeling of the fiber sheet (in the area surrounded by the white line in Fig.

Table 4 Comparison between Experiment and Calculation in this Paper

Specimen	Type of fiber sheet	Angle of crack	Maximum load (kN)	Shear capacity of fiber sheet	
				Experiment (kN)	Calculation (kN)
96-S-N	-	-	16.8	-	-
96-S-A	AFS96	45.6	31.4	14.6	16.4
96-S-C	CFS96	45.6	28.5	11.7	14.3
97-S-N	-	-	47.6	-	-
97-S-A	AFS97	37.8	69.9	22.3	20.9
97-S-C	CFS97	35.9	91.7	44.1	33.3
97-S-N-H	-	-	48.3	-	-
97-S-A-H	AFS97	35.2	68.5	20.2	12.6
97-S-C-H	CFS97	34.2	68.2	19.9	15.2

8(a) and the black line in Fig. 8(c)). The peeling process in these RC beam experiments was the same as in the model RC member experiments. Once the crack reaches the upper flange, peeling occurs from the upper edge of the fiber sheet over the crack. When the peeling reaches the half height of fiber sheet, the RC beam fails at the maximum load. The crack characteristics, as shown in Fig. 8(b) and (d), and the effective bond area, as shown in Fig. 6(a) and (c), are almost the same shape.

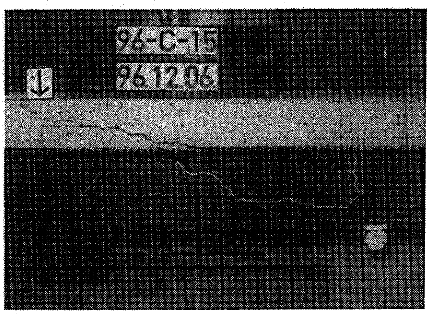

(a) Photograph of Shear Failure in 96-C-15

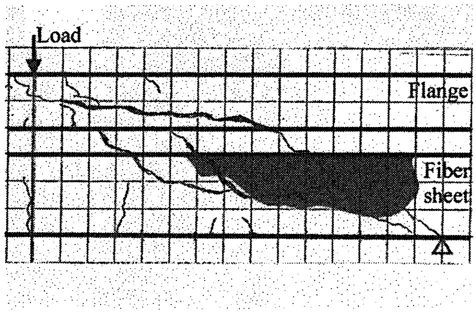

(b) Peeling Area and Crack Phenomenon in 96-C-15

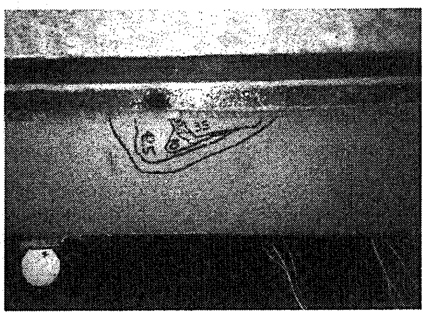

(c) Photograph of Shear Failure in 97-A-0

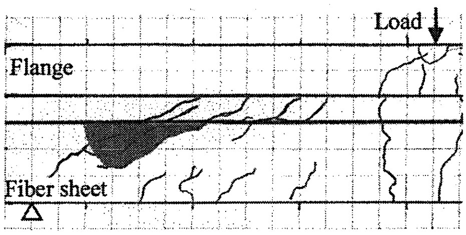

(d) Peeling Area and Crack Phenomenon in 97-A-0

Fig. 8 Shear Failure due to Peeling of Fiber Sheets

(2) Estimation of Shear Strength

In this paper, when RC beams fail due to shear cracking after the fiber sheet peels, the shear strength, V, is divided into three constituents: the shear capacity the concrete V_{cd}, the stirrups V_{sd} and the fiber sheet V_{fy}. This is shown by Eq. (3).

$$V = V_{cd} + V_{sd} + V_{fy} \tag{3}$$

V_{cd} includes coefficient β_{nt}, which takes axial stress into consideration on the basis of past research [11]. V_{sd} is calculated by truss theory.

$$\beta_{nt} = \sqrt{1 + \sigma'_{nd}/f_{td}} \tag{4}$$

Where, σ'_{nd} = average compressive stress due to axial stress (N/mm^2)
f_{td} = tensile strength of concrete (N/mm^2)

However, it is assumed that the prestressing force is distributed uniformly, and σ'_{nd} is calculated.

A comparison of the strain of the fiber sheet in orthogonal direction in gage R2 and the stirrup strain at gage S3 is shown in Fig. 9. Gages R2 and gage S3 are in almost the same location. Although there is a variation among RC beams, gage R2 is located at the half height of the fiber sheet near the vertex of the right triangle which is the effective bond area. As shown in this figure, the fiber sheet has peeled at the point where the stirrup yields; in other words, at the point where the strain of the stirrup exceeded 2000x10^{-6}. Though there were few experiments and the clarification cannot be said to be complete, when fiber sheets and stirrups are used together and the displacement of a beam progresses to the extreme after yield of the stirrups, it is clear that the fiber sheet peels because it is unable to sustain the displacement. Therefore, not all the bond capability of the fiber sheet is utilized. Once the strain of a fiber sheet exceeds 3000x10^{-6}, it peels as in Fig. 9. Compared with the load at 2000x10^{-6} and 3000x10^{-6}, it hardly increases. Therefore, it is thought that almost simultaneously with the yield of stirrups, the fiber sheet also becomes unable to carry any increment in the load. V_{fy} is calculated by Eq. (2a), (2b) and Eq. (6). Eq. (6) is the equation for bond limit strain from our past work [1].

$$V_{fy} = \frac{\varepsilon_{sy}}{\varepsilon_{p,f}} \cdot V_{fd} \tag{5}$$

Where, ε_{sy} = yield strain of stirrup (in this paper, the strain is 2000 × 10^{-6})
$\varepsilon_{p,f}$ = bond limit strain of fiber sheet

$$\varepsilon_{p,f} = (b_1 \cdot f_t + b_2) \times 10^{-6} \tag{6}$$

Where, b_1 = 1390 for AFS
b_1 = 1230 for CFS
b_2 = 2730 for AFS
b_2 = 824 for CFS
f_t = tensile strength of concrete (N/mm^2)

After the stirrups yield, the fiber sheet carries part of the increase in load which the stirrups had carried till that point. It is thought that the stirrups are unable to carry the increase in load after the stirrups yield. If the volume of stirrup reinforcement is large, the load increase which the fiber sheets must carry becomes excessive after the stirrups yield. Therefore, since the load which the fiber sheet can carry are exceeded greatly, the fiber sheet peels and RC beam fails.

If the volume of stirrup reinforcement is little, the load which the fiber sheet can carry are not exceeded after the stirrups yield and the fiber sheet does not peel simultaneously with stirrup yield. Therefore, the fiber sheet fully performs. The shear capacity of the fiber sheet is estimated by Eq. (2a) and (2b), which are the same equations as for RC members without stirrups.

Since the scope of Eq. (2a), (2b), and (5) is not clearly specified in this paper, it is a subject.

In this paper, the volume of reinforcement against shear cracking, both stirrups and fiber sheet, is shown in Table 5. A_{wr} is the sectional area of stirrups against shear cracking. A_{fr} is the sectional area of fiber sheet against shear cracking. $n \cdot A_{fr}$ is the value of A_{fr} converted into a sectional area of stirrups. These values are given as follows:

$$A_{wr} = \frac{A_w \cdot z}{s \tan \alpha} \tag{7}$$

Where, A_w = section area of one pair of stirrups (mm^2)
s = spacing between stirrups (mm)

$$A_{fr} = \frac{t_f \cdot z}{\tan \alpha} \tag{8}$$

$$n = \frac{E_w}{E_f} \tag{9}$$

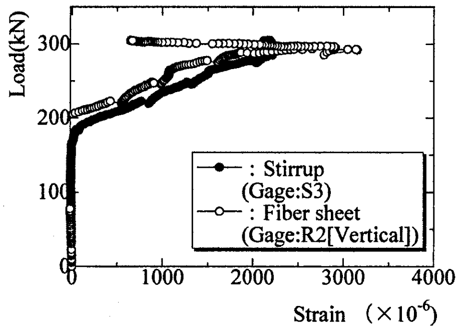

(a)96-A-0

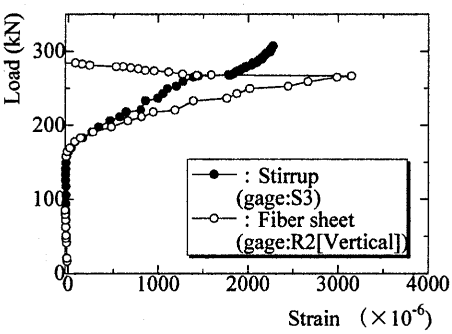

(b)96-C-0

Fig. 9 Comparison of the Strain of Fiber Sheet and Stirrups

Table 5 Sectional Area of Stirrups against Shear Crack A_{wr} and Section Area of Fiber Sheet against Shear Crack A_{fr}

Specimen	Angle of crack α	A_{wr}	A_{fr}	$n \cdot A_{fr}$	$n \cdot A_{fr}/A_{wr}$
96-C-0	31.1	108.4	76.7	92.8	0.856
96-C-15	31.4	107.2	75.8	91.7	0.856
96-A-0	29.2	117.0	106.4	45.8	0.391
96-A-15	29.3	116.6	106.0	45.6	0.391
97-A-0	26.1	133.5	142.5	52.0	0.390

As shown in the table, when $n \cdot A_{fr}/A_{wr}$ is 0.856 or less with CFS and 0.390 or less with AFS, calculation is possible by Eq. (5).

(3) Comparison Experimental and Calculated Results

The experimental results and calculated results obtained in this paper are shown in Table 6. Similar results from past research [6],[7] are shown in Table 7. Improvement in shear due to prestressing force is an increment of V_{cd} by β_{nt}.

As shown in these tables, it is possible to calculate the improvement in shear strength due to the fiber sheet and also the improvement in strength due to prestressing force using the proposed equation.

Table 6 Experimental and Calculation Result for RC Beams in this Paper

unit (kN)

Specimen	Maximum Load [Experiment]	Improvement of shear strength due to fiber sheet [Experiment]	Improvement of shear strength due to fiber sheet [Calculation]	Improvement in shear strength due to prestressing force [Experiment]	Improvement in shear strength due to prestressing force [Calculation]	Failure
96-N-0	294	-	-	-	-	S
96-C-0	307	13	15.2	-	-	PS
96-C-15	328	13	15.2	21.0	17.2	PS
96-A-0	305	11	10.3	-	-	PS
96-A-15	327	11	10.4	22.0	17.0	PS
97-N-0	409	-	-	-	-	S
97-A-0	428	19	11.9	-	-	PS

S: Shear failure; PS: Shear failure due to peeling of fiber sheet

Table 7 Experimental and Calculation Results in Past Research

Specimen	Type of fiber sheet	Young's modulus of fiber sheet (kN/mm^2)	Compressive strength of concrete (N/mm^2)	Maximum load [Experiment] (kN)	Improvement in shear strength due to fiber sheet (kN) [Experiment]	Improvement in shear strength due to fiber sheet (kN) [Calculation]
N10[6)]	-	-	30.4	247.6	-	-
N10-E100S[6)]	CFS	433	30.4	272.1	24.5	26.8
N-N-S[7)]	-	-	32.4	207.9	-	-
R1-N-S[7)]	CFS	200	32.4	225.6	17.7	24.0

5. CONCLUSION

The results obtained from this study are summarized as follows:

(1) When the fiber sheet is bonded to the web of the RC member, an effect of shear strengthening can be expected regardless of stirrups.

(2) In RC members without stirrups, the effective bond area to shear cracking was calculated. It is possible to calculate the improvement in shear strength due to fiber sheet by equation including effective bond area proposed in this paper.

(3) In RC members with stirrups, when the stirrups yield and the displacement of the RC member progresses, before reaching the bond capacity of the fiber sheet to the concrete, the fiber sheet peels from the concrete surface. Besides, it is possible to calculate the improvement in shear strength due to fiber shear by equation proposed in this paper.

(4) A strengthening effect can be expected, although it is necessary to further consider the bonding between fiber sheet and concrete, when a prestressing force is introduced into the bonded fiber sheet. It is possible to calculate the improvement in shear strength due to prestressing force by equation proposed in this paper.

ACKNOWLEDGMENTS

The authors wish to thank Mr. K. Eguchi of Sho-Bond Corporation, and Mr. S. Hata of Nihon High Strength Concrete Co., Ltd, for their generous contributions and technical support.

REFERENCE

[1] Izumo, K., Saeki, N. and Ohnuma, H., "Estimation of Bond Strength between Fiber Sheets and Concrete", JOURNAL OF MATERIALS, CONCRETE STRUCTURES AND PAVEMENTS, No.641/V-46, pp.167-178, 2000 (in Japanese)
[2] Izumo, K., Asamizu, T., Saeki, N. and Shimura, K., "Bond Behaviour of Aramid and Carbon Fiber Sheeting", TRANSACTIONS OF THE JAPAN CONCRETE INSTITUTE, Vol.20, pp.269-278, 1998
[3] Uji, K.: "Improvement of Shear Capacity of Existing Reinforced Concrete Members with Sheet Type Carbon Fibre Reinforcement", CONCRETE RESEARCH AND TECHNOLOGY JAPAN CONCRETE INSTITUTE, Vol.3, No.2, pp.37-47, 1992 (in Japanese)
[4] UMEZU, K., FUJITA, M., NAKAI, H. and TAMAKI, K., "Shear Behavior of RC Beams with Aramid Fiber Sheet", Proceeding of Symposium on Application of Advanced Reinforcing Materials to Concrete Structure, JCI Hokkaido Chapter, pp. 125-132, 1996 (in Japanese)
[5] SATO, Y., TANAKA, T., UEDA, T. and ONO, S., "Shear Reinforcing Effect of Carbon Fiber Sheet Attached to Side of Reinforced", Proceeding of Symposium on Application of Advanced Reinforcing Materials to Concrete Structure, JCI Hokkaido Chapter, pp. 133-140, 1996 (in Japanese)
[6] KATO, H., KOJIMA, T., TAKAGI, N. and HAMADA, Y., "Experimental Study on Shear Reinforcement of RC beams by Using Carbon Fiber Sheet", Proceeding of the Japan Concrete Institute, Vol.18, No.2, pp.101-106, 1996 (in Japanese)
[7] Sueoka, H., Sano, K., Majima, M. and Okano, H., "Effect of shear strengthening RC members with fiber sheet", PROCEEDINGS OF THE 51TH ANNUAL CONFERENCE OF THE JAPAN SOCIETY OF CIVIL ENGINEERS, 5, pp.944-945, 1996 (in Japanese)
[8] Sekijima, K., Kigure, A., Suzuki, H. and Ohtsuka, Y., "Study on Retrofitting Method for Concrete Members by Prestressing with Fiber Reinforced Plastics (FRP) Plate", TECHNICAL RESEARCH REPORT OF SHIMIZU CORPORATION, Vol.62, pp115-124, 1995 (in Japanese)
[9] Meier, U., Deuring, M., Meier, H. and Schwegler, G., "Strengthening of Structures with CFRP Laminates", Research and Application in Switzerland, Canadian Society of Civil Engineering, 1992
[10] SAEKI, N., TAKADA, N. and FUJITA, Y., "Resistance of Reinforced Concrete Member Subjected to Torsion", JOURNAL OF MATERIALS, CONCRETE STRUCTURES AND PAVEMENTS, No.390/V-8, pp.123-130, 1988 (in Japanese)
[11] NIWA, J., YAMADA, K., YOKOZAWA, K. and OKAMURA, H., "Revaluation of the Equation for Shear Strength of Reinforced Concrete Beams without Web Reinforcement", JOURNAL OF MATERIALS, CONCRETE STRUCTURES AND PAVEMENTS, No.372/V-5, pp.167-176, 1986 (in Japanese)
[12] SAKAMOTO, Y., TAMURA, S., SUEOKA, E. and MASHIMA, M., "Study on the Effect of Continuous Fiber Sheet for Shear Reinforcement to RC Beams", Proceeding of the Japan Concrete Institute, Vol.20, No.3, pp.1279-1284, 1998 (in Japanese)